This article has been accepted for publication in a future issue of this journal, but has not been fully edited. Content may change prior to final publication. Citation information: DOI 10.1109/TBME.2021.3115799, IEEE Transactions on Biomedical Engineering

Design a novel BCI for neurorehabilitation using concurrent LFP and EEG features: a case study

Zhao Feng, Yi Sun, Linze Qian,Yu Qi*, Yueming Wang, *Member, IEEE*, Cuntai Guan, *Fellow, IEEE*, Yu Sun*, *Senior Member, IEEE*

***Abstract*— *Objective:* Brain-computer interfaces (BCI) that enables people with severe motor disabilities to use their brain signals for direct control of objects have attracted increased interest in rehabilitation. To date, no study has investigated feasibility of the BCI framework incorporating both intracortical and scalp signals. *Methods:* Concurrent local field potential (LFP) from the hand-knob area and scalp EEG were recorded in a paraplegic patient undergoing a spike-based close-loop neurorehabilitation training. Based upon multimodal spatio-spectral feature extraction and Naïve Bayes classification, we developed, for the first time, a novel LFP-EEG-BCI for motor intention decoding. A transfer learning (TL) approach was employed to further improve the feasibility. The performance of the proposed LFP-EEG-BCI for four-class upper-limb motor intention decoding was assessed. *Results:* Using a decision fusion strategy, we showed that the LFP-EEG-BCI significantly ($p < 0.05$) outperformed single modal BCI (LFP-BCI and EEG-BCI) in terms of decoding accuracy with the best performance achieved using regularized common spatial pattern features. Interrogation of feature characteristics revealed discriminative spatial and spectral patterns, which may lead to new insights for better understanding of brain dynamics during different motor imagery tasks and promote development of efficient decoding algorithms. Moreover, we showed that similar classification performance could be obtained with few training trials, therefore highlighting the efficacy of TL. *Conclusion:* The present findings demonstrated the superiority of the novel LFP-EEG-BCI in motor intention decoding. *Significance:* This work introduced a novel LFP-EEG-BCI that may lead to new directions for developing practical neurorehabilitation systems with high detection accuracy and multi-paradigm feasibility in clinical applications.**

This work was funded by the National Natural Science Foundation of China (81801785, 82172056), the grants from the Zhejiang Lab (2019KE0AD01), the Fundamental Research Funds for the Central Universities (2020FZZX01-005). This work was supported in part by the National Key R&D Program of China (2018YFA0701400) and Zhejiang University Global Partnership Fund (100000-11320). (Zhao Feng and Yi Sun contributed equally to this work. *, *Corresponding author: Yu Qi, and Yu Sun.*)

Z. Feng and L. Qian are with the Key Laboratory for Biomedical Engineering of Ministry of Education of China, Department of Biomedical Engineering, Zhejiang University, Hangzhou 310027, Zhejiang, China.

Yi Sun is with the Department of Neurology, Sir Run Run Shaw Hospital, Zhejiang University School of Medicine, Hangzhou 310020, Zhejiang, China.

Y. Qi is with the Ministry of Education Frontier Science Center for Brain Science and Brain-machine Integration, and the College of Computer Science and Technology, Zhejiang University, Hangzhou 310058, China (email: qiyu@zju.edu.cn).

Y. Wang is with the Qiushi Academy for Advanced Studies (QAAS), and the College of Computer Science and Technology, Zhejiang University, Hangzhou 310027, China.

C. Guan is with the School of Computer Science and Engineering, Nanyang Technological University, 639798, Singapore.

Yu Sun is with the Key Laboratory for Biomedical Engineering of Ministry of Education of China, Department of Biomedical Engineering, Zhejiang University, Hangzhou 310027, Zhejiang, China, and also with the Zhejiang Lab, Hangzhou 311121, Zhejiang, China, and also with the Department of Neurology, Sir Run Run Shaw Hospital, Zhejiang University School of Medicine, Hangzhou 310020, Zhejiang, China (email: yusun@zju.edu.cn).

***Index Terms*— Brain Computer Interface, Motor Imagery, Common Spatial Pattern, Transfer Learning, Rehabilitation**

I. INTRODUCTION

Instead of the conventional neuromuscular pathways, brain-computer interface (BCI) enables people to directly interact with external environment through brain signals [1]. Such characteristics have attracted continuously growing interest in applying BCI in the field of rehabilitation. Specifically, BCI could decode the motor intentions of patients suffering from severe motor disabilities into control signals of external devices, which have been proved to promote neural plasticity through neurofeedback [2]–[5]. In fact, one of the advantages of the BCI-based motor rehabilitation approach over traditional therapy (e.g., physiotherapist therapy, constrained-induced movement therapy) is the patient-oriented close-loop training paradigm that stimulates the motivation and does not require remaining residual movement of paralyzed limbs [6]. Accumulating clinical studies have reported encouraging outcomes in motor recovery through utilizing BCI approaches. For instance, a recent review reported that state of the art controlled clinical researches on BCI-based therapies for stroke motor rehabilitation achieved higher clinical scores than the controlled condition [7]–[9]. Despite these promising results, obstacles still remain for the wide applications of BCI-based rehabilitation, including the task-oriented and subject-oriented design of paradigms, the detection accuracy for users' motor intentions, the real-time signal processing methods and the stability of the systems across different training sessions and/or subjects [10]–[13]. Additional efforts are therefore needed to develop novel BCI paradigms to further improve the practicability toward more effective rehabilitation systems.

BCI decodes users' intentions from various brain signals that could be categorized into invasive BCI and non-invasive BCI [14]. Among non-invasive BCI, electroencephalogram (EEG)-based BCI (EEG-BCI) is the most widely used method in stroke rehabilitation due to its low-cost, easy-to-use, flexible regions-of-interest (ROI) configuration, and adaptive to multiple experiment paradigms. For instance, in our recent work, we reported that 103 out of 125 stroke patients could successfully modulate EEG oscillation to use BCI neurorehabilitation system, demonstrating the clinical practicability of EEG-BCI for stroke rehabilitation [15]. However, the fact that there exists so-called EEG-BCI illiteracy (about 20% of subjects) who can't control BCI using EEG signals [16], [17] may impede the wide application of EEG-BCI technology. In addition, EEG signals are easily contaminated by different types of artifacts [18], which may lead to low decoding accuracy and affect the real-time feedback results. In comparison with non-invasive BCI, invasive BCI that decode users' intentions from intracortical brain signals (e.g., local field potential (LFP) and spike) is less affected by noise and have already demonstrated its feasibility in detecting intentions of paraplegic patients to directly control assistive tools [19]–[25].

However, the long-term usage of spike signals is of concern due to the tissue reaction that could lead to gradually reduced signal quality over time [26] while the LFP signals were more stable than the spike [27], [28]. Moreover, the intracortical acquisition system requires careful pre-surgery calibration and location determination that could not be easily modified once implemented. To date, no study has developed a BCI system incorporating both intracortical and scalp signals that could inherit advantages of long-term usage and high signal quality (LFP-BCI) as well as flexible ROI configuration and multi-paradigm extensibility (EEG-BCI) to further improve the feasibility of BCI in neurorehabilitation.

Applying BCI technology typically requires careful calibration of the decoding model at the beginning of each session, which may take a long time and make it inconvenient for patients to use [29]. Recent work has suggested that transfer learning (TL) methods could contribute to a short-time calibration thereby improving the practicability of the BCI in rehabilitation [30] [31]. Heuristically, TL learns the prior knowledge from source domain that usually contains sufficient labeled data from relative conditions (i.e., data collected from other subjects or from previous sessions of the same subject) to reduce the calibration effort for the target tasks [32]. Several recent attempts have been made to use the regularized common spatial pattern (CSP) framework for TL to improve the calibration efficiency [33]. The regularized CSP finds common information in EEG signals to construct robust spatial filters [34], [35], which could be applied to extract task-relative features from source domain data to facilitate decoding of the target task. Specifically, in a recent study [36], Cho et al., employed the regularized CSP-based TL for a two-class motor imagery (MI) classification and found that the proposed session-to-session TL strategies could achieve comparable performance without prior calibration for a new session. More recently, Jayaram and colleagues introduced a TL framework that was capable of using cross-subject and cross-session shared data structure and demonstrated its utility in MI detection of a patient with amyotrophic lateral sclerosis [32]. In sum, TL method has already demonstrated its superiority in BCI-related neurorehabilitation and further development of TL could contribute towards practical and user friendly rehabilitation systems [37].

Taking into account all of the above, we proposed a novel BCI for neurorehabilitation that utilized concurrent LFP and EEG signals (named LFP-EEG-BCI) and assessed its performance with data collected from a paraplegic patient as he went through spike-based close-loop neurorehabilitation training, where a desktop-based virtual reality (VR) program was used to guide MI tasks with a bilateral upper-limb exoskeleton providing feedback according to the decoding results of spike signals. The primary objective of this study was to explore the feasibility of motor intention decoding using both LFP and EEG signals, which may contribute to a practical BCI-based rehabilitation system with high decoding accuracy and long-term usability. To this end, the power features of LFP and EEG from multiple frequency bands were extracted using the regularized filter-bank CSP method and Naive Bayes models were trained to decode motor intentions. A decision fusion strategy was then applied to further improve the decoding performance. Moreover, TL approach was employed to reduce the calibration effort and improve the usability of the proposed LFP-EEG-BCI. To the best of our knowledge, this is the first attempt that utilizes intracortical LFP and scalp EEG signals to decode motor intentions. The novel BCI developed in this study may provide new insights toward effective and practical neurorehabilitation approaches.

II. Materials And Methods

A. Participant

In the current work, the volunteer participant is a 72-year-old male who suffers from completely tetraplegic (ASIA impairment scale A) following a traumatic cervical spine injury at C4/C5 level. The participant was implanted with two 96-channel Utah intracortical microelectrode arrays (4 mm $\times$ 4 mm, Utah Array with 1.4 mm length, Blackrock Microsystems, Salt Lake City, UT, USA) in the left primary motor cortex, with one array in the middle of hand knob area (array-A) and the other located medially about 2 mm apart (array-B). The signals from array-A were used in this study. The study was approved by the Medical Ethics Committee of The Second Affiliated Hospital of Zhejiang University (Ref. 2019-158) and was registered in Chinese Clinical Trial Registry (Ref. ChiCTR2100050705). The informed consent was obtained both verbally from the participant and his immediate family members and signed by his legal representative.

B. Experimental Protocol

Fig. 1 presents the experimental protocol for neurorehabilitation. The participant sat in a comfortable chair that supported his back and head in front of a computer monitor. A bilateral upper-limb exoskeleton with one degree of freedom at the elbow part were placed on both left and right arms of the participant. A customized desktop-based VR program with two virtual arms presented in the first-person perspective was used to carry out rehabilitation training. At the beginning of each trial, a text cue of “准备” (which means get ready for the MI tasks) appeared on the screen with an auditory notice, indicating that the participant should prepare to perform MI task. After 1 s the text changed to the name of motor tasks to be performed (including left elbow flexion, right elbow flexion, both elbow flexion, and rest), and the virtual arms executed the corresponding movement for 2 s. Then the text changed (including left elbow extension, right elbow extension, both elbow extension, and rest) and the virtual arms acted for 1 s. The patient was told to continue performing MI following the virtual arms until the text changed to “结束” (which means the end of the MI tasks) with an auditory notice, and the exoskeleton drove the arms to complete the action according to decoding results of spike signal to provide neurofeedback. Specifically, the first 8 trials of each session (2 trials per task) were used for the calibration of the spike-based classifier, which was applied for the following online decoding of motor intentions of the patient. The exoskeleton was triggered to provide sensorimotor feedback once the intentions were correctly decoded and concurrent LFP and EEG signals from the close-loop training trials were used for the following offline analysis. Each session consists of 40 trials (10 trials per task) and the participant took part in two sessions each day. Signals from two days (i.e., Day1, Day2) with an interval of two weeks were used in this study.

C. Data Acquisition and Preprocessing

In this study, EEG and LFP were recorded simultaneously during the rehabilitation training.

1) EEG: EEG data were collected from 55-scalp electrodes according to the international 10-20 system through a wireless system (model: NeuSen W, Neuracle, China). Among the 55 channels, 3 were excluded to make space for the LFP recording setup. The raw EEG signals were sampled at 1000 Hz with reference of CPz. Electrode impedance was kept below 10 kΩ throughout the recording. A standard EEG preprocessing pipeline was adopted using EEGLAB toolbox [38], which includes band-pass filter into [1, 40] Hz, re-reference to the common average reference, bad epochs exclusion and independent component analysis (ICA) [39] for artifacts removal. After that, the preprocessed EEG data were down-sampled to 250 Hz for the following analysis.

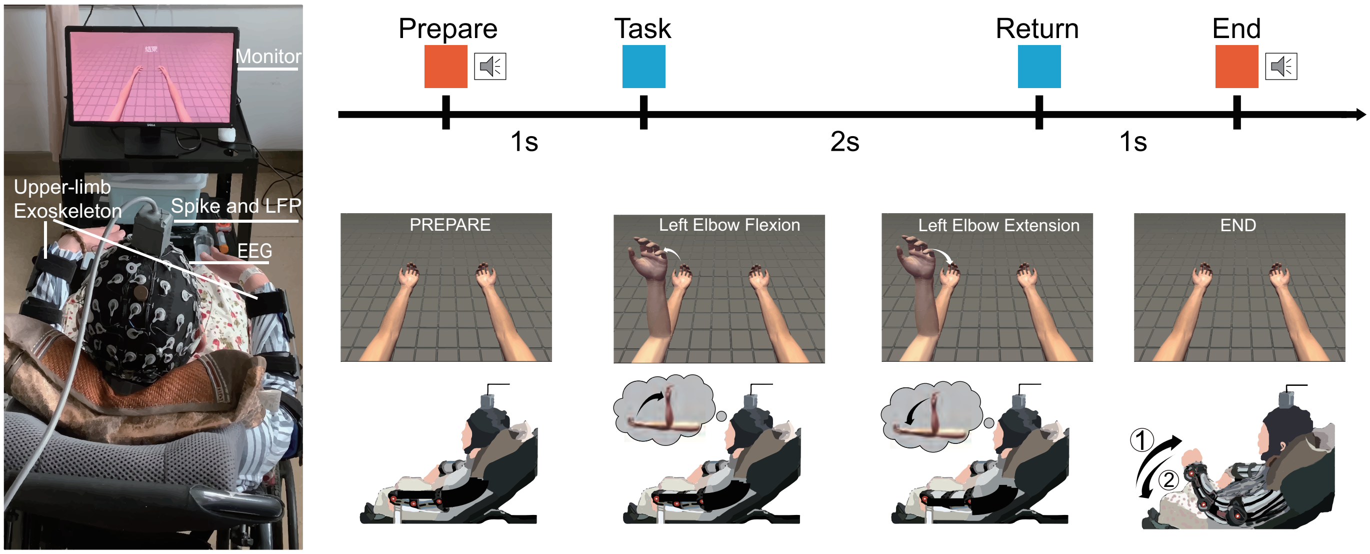

Fig. 1. Experimental protocol of neural rehabilitation training. A desktop-based VR program is used to guide motor imagery tasks. Intracortical signals (spike and LFP signals) and EEG were collected simultaneously, where the spike signals were used to decode motor intention of the patient and the outputs were set the trigger for controlling a bilateral up-limb exoskeleton that is used to provide sensorimotor feedback.

TABLE I
NUMBER OF INCLUSION TRIALS USED IN THIS STUDY

	Left	Right	Both	Rest	Total
Day 1	31	27	27	33	118
Day 2	30	28	28	36	122

2) LFP: LFP data were collected from 96 channels using a Utah array placed in the middle of the hand knob area. The sample rate was set at 1000 Hz. The preprocessing of LFP signals includes zero-phase band-pass filter into [1, 200] Hz and bad epochs exclusion. Here, only epochs with good signal quality for both EEG and LFP were included for the following analysis. In Tabel I, we showed the details of data sets used in this study.

D. Feature Extraction and Classification

The CSP method [40] that has been proved to effectively capture the event-related desynchronization/synchronization (ERD/ERS) characteristics of MI was utilized to extract features of EEG and LFP. Mathematically, CSP tried to find a spatial filter w that maximizes the following function:

$$J(w) = \frac{w^T C_1 w}{w^T C_2 w}, \tag{1}$$

where C_i was the covariance matrix from class $i \in [1, 2]$. However, the original CSP was sensitive to various noise and may suffer from the overfitting problem if a small training set was used [41]. Recent studies showed that regularization could improve the robustness of CSP features [34]. Here, two previously-validated regularized-CSP methods: shrinkage-regularized CSP (SRCSP) [42] and Tikhonov-regularized CSP (TRCSP) [43] were adopted. The objective function of the SRCSP was [42]:

$$J(w) = \frac{w^T \bar{C}_1 w}{w^T \bar{C}_2 w}, \tag{2}$$

$$\bar{C}_i = (1-\lambda)C_i + \lambda I \quad i \in [1, 2], \tag{3}$$

where λ was the regularization parameter that has a closed-form analytical solution using oracle approximating shrinkage estimator, which performed well in small sample data sets under Gaussian distribution [44].

The objective function of the TRCSP is [41]:

$$J(w) = \frac{w^T C_1 w}{w^T C_2 w + \alpha P(w)}. \tag{4}$$

The regularization parameter α and $P(w)$ in this work was set according to [42] (α=1×10^{-4} and $P(w) = w^T w$) .

In order to extract power oscillation in different brain rhythms effectively, a filter-bank approach was used [45], [46]. For EEG data, signals from 19 electrodes (including FC5, FC3, FC1, FC2, FC4, FC6, C5, C3, C1, Cz, C2, C4, C6, CP5, CP3, CP1, CP2, CP4 and CP6) overlaying the motor cortex were used for further analysis. Then, EEG data were bandpass filtered into 17 frequency bands (center frequency from 4 Hz to 36 Hz with bandwidth of 4 Hz and 50% overlapped). We used a 1 s EEG epoch (X_{EEG}, [0.5, 1.5] s after the beginning of MI tasks) for feature extraction. Since the CSP method was designed for binary classification, *one-vs-one* approach was used to extract features to distinguish four-class MI tasks, resulting in $C_4^2 = 6$ spatial filter matrixes W_{EEG} per frequency band. The first and last two columns were selected and ended up with 408 (4 $\times$ 6 $\times$ 17) features. The CSP features F_P (p = 1, 2, 3, & 4) were calculated as:

$$F_p = log[var(W_{EEG}^T(:,p) \times X_{EEG})] \tag{5}$$

Likewise, LFP data were initially filtered into 7 frequency bands (i.e., δ: $1-4$ Hz, θ: $4-8$ Hz, α: $8-13$ Hz, β: $13-30$ Hz, low-γ: $30-50$ Hz, medium-γ: $50-100$ Hz, and high-γ: $100-200$ Hz). The same 1 s epoch (X_{LFP}, [0.5, 1.5] s after the beginning of MI tasks) was used to calculate 168 (4 $\times$ 6 $\times$ 7) features with spatial filters W_{LFP}:

$$F_p = log[var(W_{LFP}^T(:,p) \times X_{LFP})] \tag{6}$$

For each signal, feature selection was performed based on the Pearson correlation between features and training labels. The selected features and their corresponding labels $L \in$ [*Rest*, *Left Hand*, *Right Hand*, *Both Hand*] were then used to train a Naive Bayes classifier with an assumption of Gaussian distributed data. In order to assess the generalization ability of different CSP methods, we performed 25

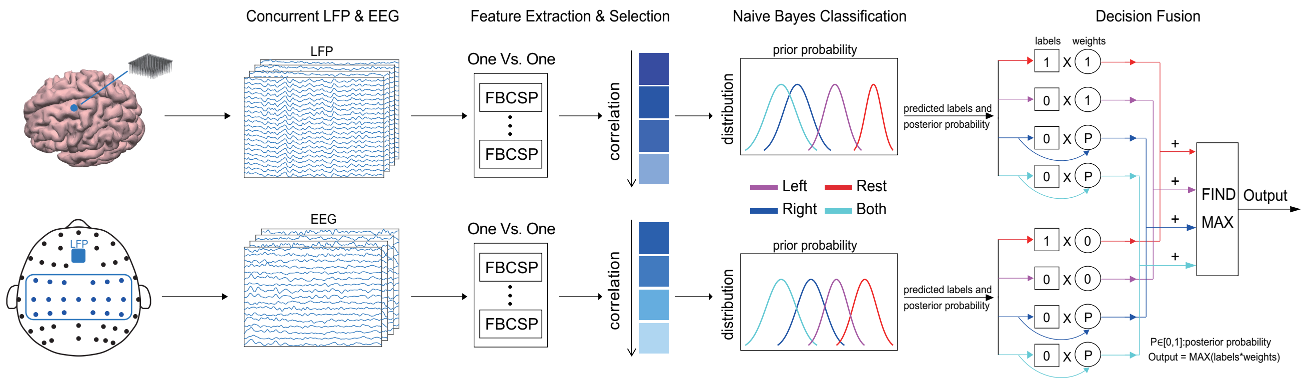

Fig. 2. The workflow of proposed framework. The LFP signals from left hand knob area and EEG signals were collected simultaneously and EEG data from regions of interest were used for analysis. The CSP filters were used to extract the multi-frequency power features of LFP and EEG. Then a correlation-based method was used to select task-relative features and Naive Bayes models were trained for decoding LFP features and EEG features separately. A decision fusion strategy was applied to vote for final results based on the predicted results and posterior probability from Bayes classifiers.

times of 5-fold cross-validation for the four-task MI classification.

E. Decision Fusion

Since the LFP and EEG signals encoded motor intention in different aspects, a decision fusion strategy was applied to combine information from both EEG and LFP signals to further improve the classification performance. Specifically, the trained Bayes models were used to get the predicted results of LFP features and EEG features. Let $P_{LFP}/P_{EEG} \in [0,1]$ being the posterior probability and L_{LFP}/L_{EEG} being the predicted labels, the final results L were calculated as:

$$L = \begin{cases} L_{LFP}, & P_{LFP} \geq P_{EEG} \\ L_{EEG}, & P_{LFP} < P_{EEG}. \end{cases} \tag{7}$$

Here, we set $P_{LFP} = 1$, if L_{LFP} was *Rest* (abbreviated as *Rt* hereafter) or *Left Hand* (abbreviated as *LH* hereafter) given that the LFP features were significantly outperformed EEG features during distinguishing these two tasks; while EEG features were used to improve the classification performance in the condition of *Right Hand* (abbreviated as *RH* hereafter) and *Both Hands* (abbreviated as *BH* hereafter) tasks. The workflow of the proposed analysis framework is illustrated in Fig. 2.

F. Feature Visualization

In order to better understand the spectral and spatial properties of brain activity during different MI tasks, the most discriminative CSP filters of LFP and EEG as well as the proportion of selected features within each frequency band were assessed. The CSP filters were thought to reflect the importance of the channels [47], which indicated whether the channels were active during MI tasks. The most important features contributing to the classification model were determined as the CSP filters that were most frequently selected during the cross-validation (e.g., in at least 80% of the iterations). Since the CSP filters are data-driven and may vary with different training trials being selected, a normalization strategy was applied to yield robust spatial filters. We first took the absolute values of CSP filters and normalized them into the range of [0, 1], then the normalized vectors were averaged through all the cross-validation cases. Thus, the values of normalized filters lie in [0, 1], with a larger value indicating a greater importance of the corresponding channel.

G. Transfer Learning

TL has shown its superior in reducing the number of calibration trials and enhancing the classification performance. Here, the regularized CSP framework for TL (TLRCSP) [35] was employed to further improve the practicability of the proposed LFP-EEG-BCI. Specifically, the multi-modal electrophysiological data of Day 1 were set as the source domain and the data of Day 2 were set as the target domain. The objective function of TLRCSP is:

$$J(w) = \frac{w^T C_1 w}{w^T C_2 w + \lambda P(w)}, \tag{8}$$

where C_1, C_2 were calculated using the source domain data and training trials of the target domain data, and λ is a user-defined regularization term, which is set as 1 manually in this study. The penalty term $P(w)$ was introduced to measure the difference between covariance of source domain data (C_s) and target domain data (C_t), which could be calculated as follow:

$$P(w) = w^T |(C_s - C_t)| w. \tag{9}$$

The idea of $P(w)$ was to seek spatial filters that could minimize the difference between C_s and C_t while maximizing the difference of variances of two classes. However, Eq. (9) could not be solved directly with Rayleigh quotient and the upper bound of $|C_s - C_t|$ was minimized instead. Specifically, for symmetric matrix $M = U diag(V_i) U^T$, the upper bound $\Gamma(M)$ was defined as:

$$\Gamma(M) = U diag(|V_i|) U^T = U|V|U^T, \tag{10}$$

such that $|\Gamma(M)| \geq |M|$. Then the new penalty term $P(w)$ was calculated as:

$$P(w) = w^T \Gamma(C_s - C_t) w, \tag{11}$$

$$\Gamma(C_s - C_t) = U|V|U^T, \tag{12}$$

$$UVU^T = C_s - C_t. \tag{13}$$

The training data of the target domain were randomly selected to construct spatial filters with the source domain trials and filter-bank CSP features were calculated as mentioned above. Feature selection was based upon the correlation between features of training trials of the target domain and the corresponding labels. After that, features of the source domain and target trials were used to train a Naive Bayes classifier. Five-fold cross-validation was repeated 5 times to validate classification performance. The framework of TL was shown in Algorithm 1. We randomly selected 10%, 20%, 50% of target data as training trials to validate the efficiency of transfer learning. The results of the non-transfer method were also calculated (i.e., the spatial filters were constructed using selected target trials by Eq. (4) and training the classifier using features of target trials) for comparison. The random selection was repeated 25 times and the averaged classification results were used to validate the performance of TL.

Algorithm 1 Transfer Learning

Input:
source domain data: $\{D_S\}_n, n = 1, 2.., N$
target domain training data: $\{D_T\}_m, m = 1, 2, .., M$
$L_S/L_T \in [1, 2, 3, 4]$: training labels of source/target domain
Output:
The trained Naive Bayes model
Begin
Compute $C_s = \frac{1}{N}\sum_n cov(\{D_S\})$
Compute $C_t = \frac{1}{M}\sum_m cov(\{D_T\})$
for l = 1:4 **do**
Find $D_{Sl} \in D_S$ and $D_{Tl} \in D_T$ with $L_S/L_T = l$
Compute $C_l = \frac{1}{Nl}\sum_{nl} cov(\{D_{Sl}\}) + \frac{1}{Ml}\sum_{ml} cov(\{D_{Tl}\})$
end for
1) Construct spatial filters W_s by Eq. (8), Eq. (11)–(13)
2) Calculate features of D_T as F_T by Eq. (5) and Eq. (6)
3) Select features according to the correlation between F_T and L_T. Get spatial filters $w \in W_s$ that yield these features
4) Calculate features of D_S as F_S using w by Eq. (5) and Eq. (6). Train Naive Bayes classifier using $\{F_T, L_T\}$ and $\{F_S, L_S\}$
End

III. Results

A. Performance of Different CSP Methods

To assess the performance of various CSP methods (Fig. 3), separate one-way ANOVA with the types of CSP as the factor was used in two days. The ANOVA of classification performance revealed that there existed significant differences between different LFP features ($F_{1,3}$ = 252.79, p < 0.001 for Day1 and $F_{1,3}$ = 181.53, p < 0.001 for Day2) while no significant difference was observed for the EEG features. Post-hoc analyses were performed using paired-sample t-test. For LFP signals, the performance of both regularized CSP (SRCSP/TRCSP) was significantly better (p < 0.01) than that of CSP. Between both regularized CSP methods, we found that the TRCSP method outperformed the SRCSP method (t_{124} = 9.199, p < 0.001 for Day1; t_{124} = 1.783, p = 0.077 for Day 2). Therefore, the TRCSP method was used for further analysis.

B. Performance of Decision Fusion

From Fig. 3, we showed the classification performance through utilizing single modal data and found that both LFP and EEG features achieved classification accuracy higher than the chance level with the best performance obtained using the TRCSP method. More importantly, we found that the proposed hybrid-decoding model significantly (p < 0.05 for both LFP and EEG in two days) outperformed the single modal model (Table II). Particularly, the data fusion method utilized EEG features to improve the classification result of RH $vs.$ BH tasks of LFP features showed that the mean accuracy was 4.44% higher than that of LFP features (t_{24} = 2.678, p = 0.013) for Day1 and 2.86% (t_{24} = 2.649, p = 0.014) for Day2, which lead to the superior classification results in the LFP-EEG model.

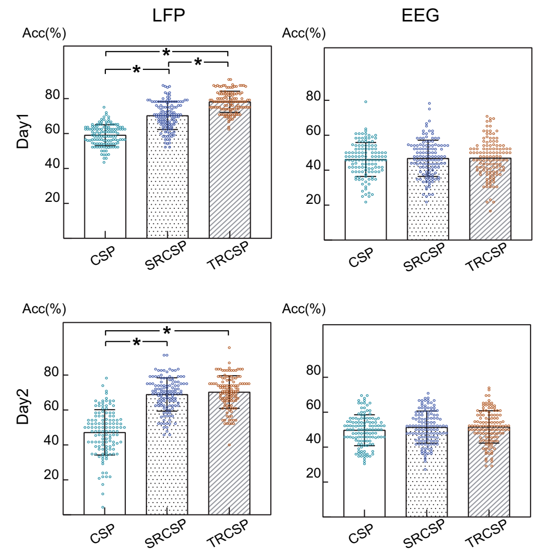

Fig. 3. Comparison of classification accuracy using different CSP methods. The TRCSP achieved the best performance for LFP feature extraction. ∗: p<0.01 (paired-sample t-test)

TABLE II
CLASSIFICATION RESULTS OF FOUR-CLASS MI TASKS

	Mean Accuracy ± Standard Error (%)		
	EEG	LFP	Fusion
Day1	54.24±2.16	79.49±2.50	81.53±3.26
Day2	50.49±4.58	73.77±2.90	75.08±2.76

C. Properties of LFP and EEG

We then interrogated the spatial and spectral characteristics of the most contributed features during various MI tasks. Specifically, 25 LFP features and 30 EEG features were selected based on the cross-validation results.

1) LFP: For the normalized filters of Rt $vs.$ MI tasks, we observed a value of 1 for Channel-71 and values below 0.25 for other channels. We observed a value of 1 for Channel-65 in the LH $vs.$ BH case while we found a value of 1 for Channel-36 in the LH $vs.$ RH case. As for the normalized filters of RH $vs.$ BH, we found a value close to 0.97 for Channel-5 and a value around 0.69 for Channel-7 (Fig. 4(a)). Moreover, most of the selected features were from β and γ frequency bands. Specifically, features from β, medium-γ and high-γ oscillation were used to differentiate Rt and MI tasks. On the other hand, γ rhythms contained the main difference of LFP features between different MI tasks.

2) EEG: Although the normalized filters of Rt $vs.$ MI tasks exhibited similar spectral pattern, that is the most contributing features were from low frequency bands (including δ, θ, α and low-β), the spatial patterns were complex across three classification models (Fig. 4(b)). Specifically, the spatial patterns of Rt $vs.$ LH filter got high values around Channel C1 and C5; with Rt $vs.$ RH showed high values around Channel FC3 and CP3; with Rt $vs.$ BH showed high values around Channel Cz and C1. Moreover, the features that differentiated various MI tasks distributed over a wide frequency spectrum. The spatial patterns of LH $vs.$ RH showed more importance at Channel Cz, C2, and CP2; with LH $vs.$ BH had high score at Cz and C1, and RH $vs.$ BH had high score at C1.

D. Performance of Transfer Learning

In Table III, we showed the feasibility of TL approach for reducing calibration trials and enhancing classification performance. Particu-

This article has been accepted for publication in a future issue of this journal, but has not been fully edited. Content may change prior to final publication. Citation information: DOI 10.1109/TBME.2021.3115799, IEEE Transactions on Biomedical Engineering

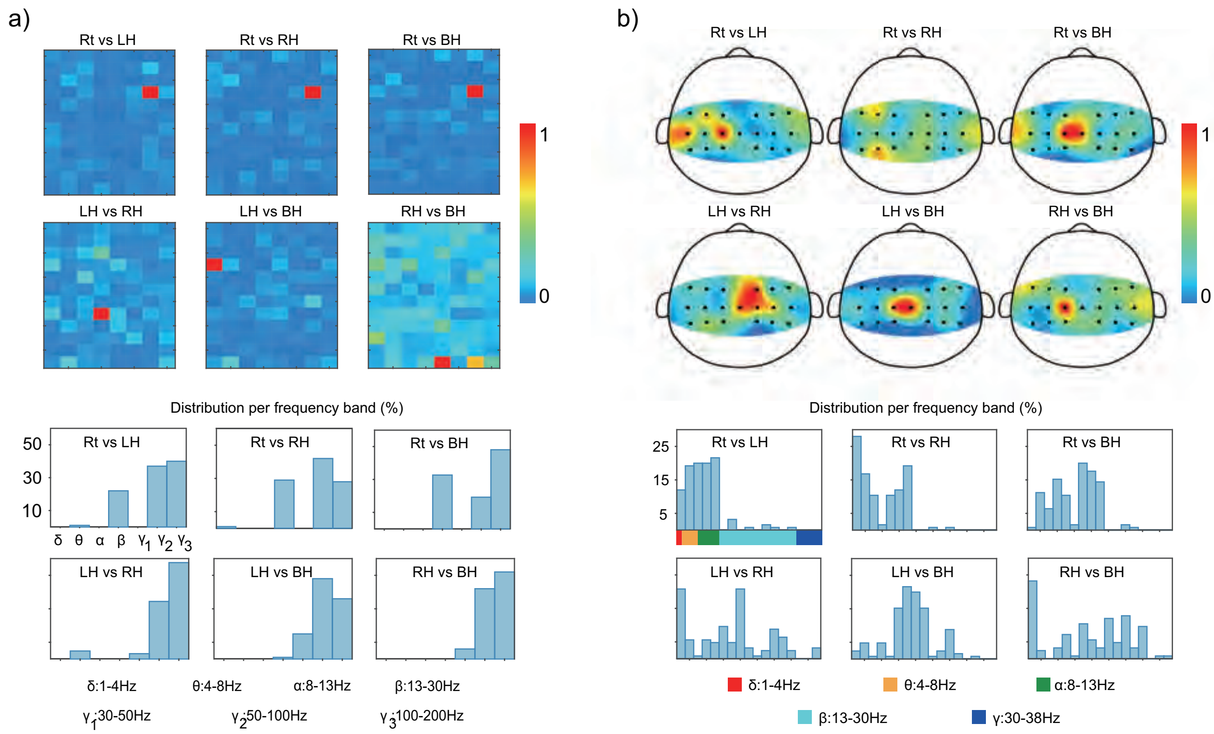

Fig. 4. The spatial weights and spectral distributions of a). *LFP features* b). *EEG features* under different motor imagery tasks. The spatial weights are normalized to [0, 1] with larger values indicating more importance of the corresponding channels. The spectral distribution illustrates the proportion of features from each frequency band.

TABLE III
CLASSIFICATION RESULTS OF TRANSFER LEARNING WITH DIFFERENT NUMBER OF TARGET TRIALS

Target Number*	Mean Accuracy ± Standard Error (%)	
	Transfer	Non-transfer
12	67.30±3.55	33.98±7.89
24	70.08±5.13	49.63±9.63
60	74.10±2.96	71.41±4.18

* note: target number is the number of training trials used for 4 tasks, e.g. 12 target number means that 3 trials of each task is used.

larly, the TL method achieved satisfactory classification rate using only 12 training target trials (that is 3 trials per class), while the non-transfer approach required much more training data to achieve the similar result. As expected, we found that the performance of TL enhanced moderately as the number of target trials increases (12 *vs.* 24, t_{124} = -1.987, p = 0.058; 24 *vs.* 60, t_{124} = -3.509, p = 0.002). Besides, the classification accuracy of TL method is significantly better than that of non-transfer case even under large number of target training trails (t_{124} = 2.871, p = 0.008 for target trials number = 60).

IV. Discussion

In the current exploratory work, we successfully built, for the first time, a novel LFP-EEG-BCI using concurrent LFP and EEG signals and assessed its performance during the neurorehabilitation training of a paraplegic patient. The significant findings are as follows: first, in comparison with the original CSP and the SRCSP method, we found that the TRCSP method could effectively extract salient power features of LFP and EEG for different MI tasks. Second, we showed that decision fusion approach through incorporating the predicted results of both LFP and EEG features significantly improved the classification performance. Third, the most contributing features of LFP and EEG for the classification models exhibited different spectral and spatial patterns. Finally, we demonstrated the efficacy of the TL method in improving the practicability of the proposed BCI. These findings are discussed in greater detail below.

A. CSP Methods for Feature Extraction

The CSP method has been widely used for feature extraction and has demonstrated its feasibility in BCI-based neurorehabilitation studies [31]. In order to improve the performance under scenarios of small training samples and prevent overfitting, various regularized versions of CSP algorithms were introduced [41]. In line with early studies [42], we found that two widely-used regularized CSP methods (i.e., SRCSP and TRCSP) outperformed the original CSP method. This finding may therefore provide new evidence to support the superiority of regularized CSP in LFP-BCI. Besides, the TRCSP achieved significantly better classification performance than SRCSP, indicating that the spatial penalty in TRCSP could effectively reveal the characteristics of brain signals with high local similarity. However, the improvement of two regularized CSP methods for EEG features failed to show statistical significance. It may be caused by the relatively low signal-to-noise ratio and the limited number of trials in EEG. It should also be aware that the patient was naive to EEG-BCI prior to the current work and no training session of modulating EEG was carried out [48], which may lead to the lower decoding performance of the EEG-BCI in comparison with the LFP-BCI. In addition, the performance of CSP methods applied in this proof-of-concept study might be affected by the nonstationarity of brain signals. More advanced CSP framework that considering the distribution of features and optimization of spatial filters selection was of interest to further improve the performance of MI detection [49].

B. Multimodal Data Fusion

The hybrid-decoding BCI aimed at measuring task-specific brain rhythms from both micro- and macro-scope. Specifically, LFP features revealed the activities of neurons, while EEG features modeled the global characteristics of the brain to provided additional information on various MI tasks. It was noteworthy mentioning that the primary objective of the current exploratory work was to take advantage of multimodal signals to achieve better decoding accuracy of motor intention for neurorehabilitation. A decision fusion strategy was employed to combine the decoding results from LFP and EEG spectral power features. Although the significantly improved decoding performance was achieved, our LFP-EEG-BCI did not make full use of the multimodal brain signals. First, additional efforts could be made to investigate feasibility through applying advanced data fusion techniques [50]–[52] and utilizing various spatio-spectral EEG features, e.g. connectivity that revealed the cooperation of various brain areas [53]. Besides, deep learning has reported promising results to extract features directly from raw EEG [54] and LFP signals [55], [56]. The fusion strategy for features extracted by deep learning approach could also be explored in future work. Moreover, the hybrid of LFP and spike has also been reported to produce better decoding performance than using single model [20], [21]. In comparison, we supposed that the superiority of our LFP-EEG-BCI over LFP-spike-BCI was the ability to incorporate multiple paradigms. The idea came from the exploration of EEG-based hybrid BCI that utilized MI-based BCI and other paradigms (e.g., P300) for multidimensional decoding [57]. Similarly, the proposed LFP-EEG-BCI could contribute to practical and self-initiated rehabilitation systems by taking advantage of multimodal brain signals, which used LFP (or hybrid spike, LFP and EEG) to decoded motor-related intentions and evoked potentials recorded by EEG to select tasks [58].

C. Most Contributing Features

The coefficients of CSP filters (spatial patterns) reflected the importance of channels [47], that is, signals recorded by channels with higher absolute values were better correlated with the tasks. Thus, the spatial patterns revealed different properties of brain activity patterns under various MI tasks. For LFP, we found that the patterns were rather robust and discriminative, with one channel having a value close to 1 and the others close to 0 for most cases. The findings were in line with [59] that reported the effectiveness of stable spatial patterns of LFP derived from CSP methods for movement directions decoding. Of note, the activity patterns derived from *RH* and *BH* tasks were less robust, which may lead to the limited classification performance of LFP-BCI. This could be attributed to the embedded information of *RH* in *BH* trials that were recorded from the leftward placed recording system. Besides, most of the features selected were from γ (>50 Hz) and β frequency bands that revealed the spectral encoding structure of LFP signals for motor-related information. These findings were consistent with the results reported in previous LFP-BCI studies, for example, the β and γ bands LFP were used for detecting patients' intention of selection [28] as well as prediction of kinematic information (e.g., movement directions) [21], [60]. Additionally, as suggested in [21], [60] that the β rhythm and γ (>50 Hz) rhythm of LFP showed a disparity of motor modulation. Specifically, the γ-LFP signals and spike were highly correlated with movement direction modulation while β-LFP contained independent information. In our study, the β rhythm played an important role in the classification of *Rt* and MI tasks only while the γ rhythm worked in all the classification cases. We therefore posited the spectral encoding structure of LFP signals that signals from γ rhythm contained information of which limb to act as well as the start of movement while β rhythm coded the movement initiation in a different way.

For EEG signal, we applied a filter-bank approach to extract subject-specific frequency features instead of using the widely explored μ and β rhythms [61]. The selected most contributing features indicated that the motor intention of *LH* mainly encoded in low-frequency signals (δ, θ, α) while low-β rhythms contained extra information related to movement intention of *RH* and *BH*. In addition, δ oscillation seemed to be most correlated with *RH* MI. The spatial patterns of EEG suggested that signals from C1, Cz, C2 channels were most relevant to elbow MI tasks, which were in line with the homunculus theory as well as previous EEG-BCI rehabilitation findings [62]. The discriminative spatial patterns and spectral properties could be utilized as prior knowledge for the future development of more effective decoding algorithms.

D. TL Improves the Practicability of the LFP-EEG-BCI

Although the TL has shown its superiority in improving the calibration efficiency and reducing the requirements of training trials, only a few studies have explored its feasibility in BCI-based studies using intracortical signals [63]. Here, we demonstrated that similar classification performance ($> 70\%$) could be achieved using only 6 training trials per class through utilizing TL in comparison with 15 training trials without the application of TL. This finding therefore provided novel evidence to support the beneficial effects of TL for BCI studies. The proposed TL method in this work required a pre-defined parameter λ to regularize the knowledge transferred from the source domain [35]. In order to assess the generalizability and demonstrate that our findings were not dependent upon the arbitrary selection of this parameter, we performed an additional analysis with different values of λ (range from 0.1 to 2) and found our main findings intact (data not show). According to [21], intracortical signals (i.e., LFP) encoded motor intentions in a similar way within a short time interval (i.e., two weeks in this work), which may lay the physiological foundation for the TL to capture task-related LFP features using data collected from previous sessions. In EEG-BCI studies, the cross-subject TL that utilizes the same task-specific EEG data from other subjects has been widely adopted and demonstrated its efficacy in the calibration [33]. Given that the participant in the current work is a quadriplegic patient, the cross-subject TL may lead to a more practical solution to improve convenience and user-friendliness. Moreover, further attempts could be made to employ a complete TL framework including data alignment, spatial filtering, feature engineering and classifier learning [64], [65] to further improve the performance of the LFP-EEG-BCI.

V. Conclusion

In this paper, we introduced a novel LFP-EEG-BCI that incorporates both intracortical LFP and scalp EEG signals and assessed its feasibility with data from a paraplegic patient. We showed that the proposed BCI significantly outperformed these two conventional single-modal BCIs (LFP-BCI, and EEG-BCI) in decoding motor intention during rehabilitation training. A CSP-based transfer learning strategy was developed to further improve the practicability of the LFP-EEG-BCI via reducing the number of training trials. To the best of our knowledge, this is the first attempt to develop a practical LFP-EEG-BCI and our findings provide some of the first quantitative insights into the effectiveness of LFP-EEG data fusion for motor intention detection. More importantly, we demonstrate that the proposed BCI may lead to new directions for developing a long-term recording-stable neurorehabilitation system for paraplegic patients.

Appendix

List of Abbreviations and Acronyms

BCI	Brain-Computer Interface
BH	Both Hand
CSP	Common Spatial Pattern
EEG	Electroencephalography
EEG-BCI	EEG-based BCI
ICA	Independent Component Analysis
LFP	Local Field Potential
LFP-BCI	LFP-based BCI
LFP-EEG-BCI	BCI using concurrent LFP and EEG
LH	Left Hand
MI	Motor Imagery
Rt	Rest condition
RH	Right Hand
SRCSP	Shrinkage-Regularized CSP
TRCSP	Tikonov-Regularized CSP
TL	Transfer Learning
TLRCSP	Regularized CSP for TL
VR	Virtual Reality

Acknowledgment

The authors are grateful to the patient and his relatives for their extraordinary enthusiasm and willingness to participate in the exploratory study. We would also like to thank Dr. Jianmin Zhang and Dr. Junming Zhu from the Second Affiliated Hospital, Zhejiang University School of Medicine, for the clinical assistance.

References

[1] B. He *et al.*, "Brain–computer interfaces," in *Neural Engineering*, pp. 131–183, Springer, 2020.
[2] N. Mrachacz-Kersting *et al.*, "Efficient neuroplasticity induction in chronic stroke patients by an associative brain-computer interface," *J. Neurophysiol.*, vol. 115, no. 3, pp. 1410–1421, 2016.
[3] A. Frolov *et al.*, "Use of robotic devices in post-stroke rehabilitation," *Neurosci. Behav. Physiol.*, vol. 48, no. 9, pp. 1053–1066, 2018.
[4] F. Pichiorri *et al.*, "Brain-computer interfaces in neurologic rehabilitation practice," in *Handbook of Clinical Neurology*, vol. 168, pp. 101–116, Elsevier, 2020.
[5] N. Mrachacz-Kersting *et al.*, "Towards a mechanistic approach for the development of non-invasive brain-computer interfaces for motor rehabilitation," *J. Physiol.*, vol. 599, no. 9, pp. 2361–2374, 2021.
[6] S. R. Soekadar *et al.*, "Brain–machine interfaces in neurorehabilitation of stroke," *Neurobiol. Dis.*, vol. 83, pp. 172–179, 2015.
[7] F. Pichiorri *et al.*, "Brain–computer interface boosts motor imagery practice during stroke recovery," *Ann. Neurol.*, vol. 77, no. 5, pp. 851–865, 2015.
[8] M. A. Cervera *et al.*, "Brain-computer interfaces for post-stroke motor rehabilitation: a meta-analysis," *Ann. Clin. Transl. Neurol.*, vol. 5, no. 5, pp. 651–663, 2018.
[9] E. López-Larraz *et al.*, "Brain-machine interfaces for rehabilitation in stroke: a review," *NeuroRehabilitation*, vol. 43, no. 1, pp. 77–97, 2018.
[10] M. S. Cameirão *et al.*, "Neurorehabilitation using the virtual reality based rehabilitation gaming system: methodology, design, psychometrics, usability and validation," *J. NeuroEng. Rehabil.*, vol. 7, no. 1, pp. 1–14, 2010.
[11] Z. Zhou *et al.*, "A novel task-oriented optimal design for p300-based brain–computer interfaces," *J. Neural Eng.*, vol. 11, no. 5, p. 056003, 2014.
[12] M. A. Lebedev *et al.*, "Brain-machine interfaces: From basic science to neuroprostheses and neurorehabilitation," *Physiol. Rev.*, vol. 97, no. 2, pp. 767–837, 2017.
[13] M. A. Khan *et al.*, "Review on motor imagery based BCI systems for upper limb post-stroke neurorehabilitation: From designing to application," *Comput. Biol. Med.*, p. 103843, 2020.
[14] U. Chaudhary *et al.*, "Brain–computer interfaces for communication and rehabilitation," *Nat. Rev. Neurol.*, vol. 12, no. 9, pp. 513–525, 2016.
[15] K. K. Ang *et al.*, "Brain–computer interface for neurorehabilitation of upper limb after stroke," *Proc. IEEE*, vol. 103, no. 6, pp. 944–953, 2015.
[16] C. Jeunet *et al.*, "Why standard brain-computer interface (BCI) training protocols should be changed: an experimental study," *J. Neural Eng.*, vol. 13, no. 3, p. 036024, 2016.
[17] X. Shu *et al.*, "Fast recognition of BCI-inefficient users using physiological features from EEG signals: A screening study of stroke patients," *Front. Neurosci.*, vol. 12, p. 93, 2018.
[18] J. A. Urigüen *et al.*, "EEG artifact removal—state-of-the-art and guidelines," *J. Neural Eng.*, vol. 12, no. 3, p. 031001, 2015.
[19] L. R. Hochberg *et al.*, "Reach and grasp by people with tetraplegia using a neurally controlled robotic arm," *Nature*, vol. 485, no. 7398, pp. 372–375, 2012.
[20] A. B. Ajiboye *et al.*, "Prediction of imagined single-joint movements in a person with high-level tetraplegia," *IEEE Trans. Biomed. Eng.*, vol. 59, no. 10, pp. 2755–2765, 2012.
[21] J. A. Perge *et al.*, "Reliability of directional information in unsorted spikes and local field potentials recorded in human motor cortex," *J. Neural Eng.*, vol. 11, no. 4, p. 046007, 2014.
[22] T. Aflalo *et al.*, "Decoding motor imagery from the posterior parietal cortex of a tetraplegic human," *Science*, vol. 348, no. 6237, pp. 906–910, 2015.
[23] C. E. Bouton *et al.*, "Restoring cortical control of functional movement in a human with quadriplegia," *Nature*, vol. 533, no. 7602, pp. 247–250, 2016.
[24] C. Pandarinath *et al.*, "High performance communication by people with paralysis using an intracortical brain-computer interface," *eLife*, vol. 6, p. e18554, 2017.
[25] F. R. Willett *et al.*, "High-performance brain-to-text communication via handwriting," *Nature*, vol. 593, no. 7858, pp. 249–254, 2021.
[26] J. C. Barrese *et al.*, "Failure mode analysis of silicon-based intracortical microelectrode arrays in non-human primates," *J. Neural Eng.*, vol. 10, no. 6, p. 066014, 2013.
[27] R. A. Andersen *et al.*, "Selecting the signals for a brain–machine interface," *Curr. Opin. Neurobiol.*, vol. 14, no. 6, pp. 720–726, 2004.
[28] T. Milekovic *et al.*, "Stable long-term BCI-enabled communication in ALS and locked-in syndrome using LFP signals," *J. Neurophysiol.*, vol. 120, no. 7, pp. 343–360, 2018.
[29] M. Arvaneh *et al.*, "Omitting the intra-session calibration in EEG-based brain computer interface used for stroke rehabilitation," in *Proc. Annu. Int. Conf. IEEE Eng. Med. Biol. Soc. EMBS*, pp. 4124–4127, IEEE, 2012.
[30] P. Wang *et al.*, "A review on transfer learning for brain-computer interface classification," in *Int. Conf. Inf. Sci. Technol., ICIST*, pp. 315–322, IEEE, 2015.
[31] F. Lotte *et al.*, "A review of classification algorithms for EEG-based brain–computer interfaces: a 10 year update," *J. Neural Eng.*, vol. 15, no. 3, p. 031005, 2018.
[32] V. Jayaram *et al.*, "Transfer learning in brain-computer interfaces," *IEEE Comput. Intell. Mag.*, vol. 11, no. 1, pp. 20–31, 2016.
[33] Z. Wan *et al.*, "A review on transfer learning in EEG signal analysis," *Neurocomputing*, vol. 421, pp. 1–14, 2021.
[34] F. Lotte *et al.*, "Learning from other subjects helps reducing brain-computer interface calibration time," in *ICASSP IEEE Int Conf Acoust Speech Signal Process Proc*, pp. 614–617, IEEE, 2010.
[35] M. Cheng *et al.*, "Regularized common spatial patterns with subject-to-subject transfer of EEG signals," *Cogn. Neurodynamics*, vol. 11, no. 2, pp. 173–181, 2017.
[36] H. Cho *et al.*, "Increasing session-to-session transfer in a brain–computer interface with on-site background noise acquisition," *J. Neural Eng.*, vol. 12, no. 6, p. 066009, 2015.
[37] L. Cao *et al.*, "An inter-and intra-subject transfer calibration scheme for improving feedback performance of sensorimotor rhythm-based BCI rehabilitation," *Front. Neurosci.*, vol. 14, 2020.
[38] A. Delorme *et al.*, "EEGLAB: an open source toolbox for analysis of single-trial EEG dynamics including independent component analysis," *J. Neurosci. Methods*, vol. 134, no. 1, pp. 9–21, 2004.
[39] T.-P. Jung *et al.*, "Removing electroencephalographic artifacts by blind source separation," *Psychophysiology*, vol. 37, no. 2, pp. 163–178, 2000.
[40] H. Ramoser *et al.*, "Optimal spatial filtering of single trial EEG during imagined hand movement," *IEEE Trans. Rehabil. Eng.*, vol. 8, no. 4, pp. 441–446, 2000.
[41] F. Lotte *et al.*, "Regularizing common spatial patterns to improve BCI designs: unified theory and new algorithms," *IEEE Trans. Biomed. Eng.*, vol. 58, no. 2, pp. 355–362, 2010.

[42] V. S. Handiru *et al.*, "EEG source space analysis of the supervised factor analytic approach for the classification of multi-directional arm movement," *J. Neural Eng.*, vol. 14, no. 4, p. 046008, 2017.
[43] F. Lotte *et al.*, "Spatially regularized common spatial patterns for EEG classification," in *Proc. Int. Conf. Pattern Recognit.*, pp. 3712–3715, IEEE, 2010.
[44] Y. Chen *et al.*, "Shrinkage algorithms for MMSE covariance estimation," *IEEE Trans. Signal Process.*, vol. 58, no. 10, pp. 5016–5029, 2010.
[45] K. K. Ang *et al.*, "Filter bank common spatial pattern (FBCSP) in brain-computer interface," in *Proc Int Jt Conf Neural Networks*, pp. 2390–2397, IEEE, 2008.
[46] Y. Zhang *et al.*, "Temporally constrained sparse group spatial patterns for motor imagery BCI," *IEEE T. Cybern.*, vol. 49, no. 9, pp. 3322–3332, 2018.
[47] Y. Wang *et al.*, "Common spatial pattern method for channel selelction in motor imagery based brain-computer interface," in *Annu Int Conf IEEE Eng Med Biol Proc*, pp. 5392–5395, IEEE, 2006.
[48] T. a. Yu, "Enhanced motor imagery training using a hybrid BCI with feedback," *IEEE Trans. Biomed. Eng.*, vol. 62, no. 7, pp. 1706–1717, 2015.
[49] J. Jin *et al.*, "Internal feature selection method of csp based on l1-norm and dempster-shafer theory," *IEEE Trans. Neural Netw. Learn. Syst.*, 2020.
[50] L.-W. Ko *et al.*, "Multimodal fuzzy fusion for enhancing the motor-imagery-based brain computer interface," *IEEE Comput. Intell. Mag.*, vol. 14, no. 1, pp. 96–106, 2019.
[51] J. Fumanal-Idocin *et al.*, "Motor-imagery-based brain-computer interface using signal derivation and aggregation functions," *IEEE T. Cybern.*, 2021.
[52] I. Kakkos *et al.*, "EEG fingerprints of task-independent mental workload discrimination," *IEEE J. Biomed. Health Inform.*, 2021.
[53] B. He *et al.*, "Electrophysiological brain connectivity: theory and implementation," *IEEE Trans. Biomed. Eng.*, vol. 66, no. 7, pp. 2115–2137, 2019.
[54] X. Zhang *et al.*, "A survey on deep learning-based non-invasive brain signals: recent advances and new frontiers," *J. Neural Eng.*, vol. 18, no. 3, p. 031002, 2021.
[55] E. Nurse *et al.*, "Decoding EEG and LFP signals using deep learning: heading truenorth," in *Annu Int Conf IEEE Eng Med Biol Proc*, pp. 259–266, 2016.
[56] H. M. Golshan *et al.*, "LFP-net: A deep learning framework to recognize human behavioral activities using brain STN-LFP signals," *J. Neurosci. Methods*, vol. 335, p. 108621, 2020.
[57] H. Yuan *et al.*, "Brain–computer interfaces using sensorimotor rhythms: current state and future perspectives," *IEEE Trans. Biomed. Eng.*, vol. 61, no. 5, pp. 1425–1435, 2014.
[58] Y. Li *et al.*, "An EEG-based BCI system for 2-D cursor control by combining mu/beta rhythm and p300 potential," *IEEE Trans. Biomed. Eng.*, vol. 57, no. 10, pp. 2495–2505, 2010.
[59] N. F. Ince *et al.*, "High accuracy decoding of movement target direction in non-human primates based on common spatial patterns of local field potentials," *PLoS One*, vol. 5, no. 12, p. e14384, 2010.
[60] D. A. Heldman *et al.*, "Local field potential spectral tuning in motor cortex during reaching," *IEEE Trans. Neural Syst. Rehabil. Eng.*, vol. 14, no. 2, pp. 180–183, 2006.
[61] B. Blankertz *et al.*, "Optimizing spatial filters for robust EEG single-trial analysis," *IEEE Signal Process. Mag.*, vol. 25, no. 1, pp. 41–56, 2007.
[62] E. Veslin *et al.*, "Decoding elbow movement with kalman filter using non-invasive EEG," in *IEEE Colombian Conf. Appl. Comput. Intell., ColCACI - Proc.*, pp. 1–6, IEEE, 2019.
[63] D. M. Brandman *et al.*, "Rapid calibration of an intracortical brain–computer interface for people with tetraplegia," *J. Neural Eng.*, vol. 15, no. 2, p. 026007, 2018.
[64] H. He *et al.*, "Transfer learning for brain–computer interfaces: A Euclidean space data alignment approach," *IEEE Trans. Biomed. Eng.*, vol. 67, no. 2, pp. 399–410, 2019.
[65] D. Wu *et al.*, "Transfer learning for motor imagery based brain-computer interfaces: A complete pipeline," *arXiv preprint arXiv:2007.03746*, 2020.